REVISTA MEXICANA DE FÍSICA S **54** (3) 63–68 DICIEMBRE 2008

Transfer reactions in the investigation of light-nuclei nucleosynthesis

V. Guimarães, O. Camargo, R. Lichtenthäler, and V. Scarduelli
Instituto de Física, Universidade de São Paulo,
P.O.Box 66318, 05389-970 São Paulo, SP, Brazil.

J.J. Kolata
Department of Physics, University of Notre Dame,
Notre Dame, Indiana, 46556, USA.

H. Amro, F.D. Becchetti, and Hao Jiang
Department of Physics, University of Michigan,
Ann Arbor, Michigan 48109-1120, USA.

E.F. Aguilera, D. Lizcano, E. Martinez-Quiroz, and H. Garcia
Instituto Nacional de Investigaciones Nucleares,
Apartado Postal 18-1027, México, D.F. 11801 México.

Recibido el 27 de febrero de 2008; aceptado el 25 de abril de 2008

Cross sections for the ^{6}Li(p,γ)^{7}Be, ^{7}Li(n,γ)^{8}Li ^{8}Li(n,γ)^{9}Li and ^{8}Li(p,γ)^{9}Be capture reactions have been investigated in the framework of the potential model. The main ingredients of the potential model are the potentials used to generate the continuum and bound-state wave functions and spectroscopic factors of the corresponding bound systems. The spectroscopic factors for the ^{7}Li$\otimes$n=^{8}Li$_{gs}$, ^{8}Li$\otimes$n=^{9}Li$_{gs}$ bound systems were obtained from a FR-DWBA analysis of neutron transfer reactions induced by ^{8}Li radioactive beam on a ^{9}Be target, while spetroscopic factor for the ^{8}Li$\otimes$p=^{9}Be$_{gs}$ bound system were obained from a proton transfer reaction. From the obtained capture reaction cross section, reaction rate for the ^{8}Li(n,γ)^{9}Li and ^{8}Li(p,γ)^{9}Be direct neutron and proton capture were determined and compared with other experimental and calculated values.

Keywords: Capture reactions; transfer reactions; spectroscopic factors.

Se hace un estudio de las secciones eficaces de las reacciones de captura para ^{6}Li(p,γ)^{7}Be, ^{7}Li(n,γ)^{8}Li, ^{8}Li(n,γ)^{9}Li y ^{8}Li(p,γ)^{9}Be en el marco de un modelo de potencial. Los principales ingredientes de este modelo son los potenciales usados para generar las funciones de onda del continuo y para los estados ligados así como los factores espectroscópicos de los sistemas ligados correspondientes. Los factores espectroscópicos de los sistemas ligados para ^{7}Li$\otimes$n=^{8}Li$_{gs}$, ^{8}Li$\otimes$n=^{9}Li$_{gs}$ fueron obtenidos del análisis con FR-DWBA de la transferencia de un neutrón del proyectil radiactivo ^{8}Li a un núcleo de ^{9}Be, mientras que para el sistema ligado ^{8}Li$\otimes$p=^{9}Be$_{gs}$, los factores espectroscópicos se obtuvieron de análisis de la transferencia de un protón. De las secciones eficaces de reacciones de captura obtenidas, se determinaron las razones de reacción de captura directa y se compararon con otros valores calculados y experimentales.

Descriptores: Reacciones de captura; reacciones de transferencia; factores espectroscópicos.

PACS: 25.60.Je; 25.40.Lw; 25.70.Hi

1. Introduction

It is very important for the astrophysics to know the reaction rate of a specific reaction at the "*Gamow Peak*". For light-nuclei nucleosynthesis, in many astrophysical environments the energy of the *Gamow Peak* is very low, in the range of few tens to at most hundreds of keVs. For many light-nuclei nucleosynthesis reactions, experimental cross sections at these very low energies are not often measurable; either because the cross sections are too small or because the combination of target+beam is not possible. A typical case is the ^{8}Li(n,γ)^{9}Li capture reaction where direct measurement is not possible because no ^{8}Li or neutron target exist. For such case, the cross sections of the capture reaction have to be obtained by indirect methods. Also, where low energy measurements are not possible , extrapolation from higher energies and/or indirect methods to determine the cross sections are usually adopted. Extrapolation from higher energy data is not straigth forward. Careful and accurate account of physically relevant information has to be considered in the description of the reaction before the extrapolation is performed. The description of the reaction requires not only information on the structure of the nuclei involved but also a clear understanding of the reaction mechanism. Indirect methods to determine capture reaction cross sections include the Coulomb dissociation method, which corresponds to the inverse temporal reaction of the capture, the reduced-width or ANC (Asymptotic Normalization Coefficient) method and potential model, where the latter two use transfer reactions as a way to get information on the non-resonant part of the capture reaction process. This will be explained in more detail in the next section. These indirect methods are very suitable to be used in association with low-energy radioactive nuclear beams.

In this work, we report the results obtained for the non-resonant part of the neutron and proton capture reactions of light nuclei; ^{6}Li(p,γ)^{7}Be, ^{7}Li(n,γ)^{8}Li, ^{8}Li(n,γ)^{9}Li and

^{8}Li(p,γ)^{9}Be in the framework of the potential model. The results for the neutron capture reactions has been published elsewhere [1], while the results for the ^{8}Li(p,γ)^{9}Be proton capture reaction are still preliminary.

Neutron and proton capture reactions involving light radioactive nuclei such as ^{8}Li and ^{8}B have been found to be important in astrophysical environments such as the inhomogeneous model for big-bang nucleosynthesis [2], the initial stage of Type II supernovae [3], and nucleosynhtesis in massive stars [4]. The inhomogeneous model for big-bang nucleosynthesis [2] has been proposed as a possible way to produce higher mass abundances for A>4 nuclei which are not well predicted by the standard big-bang model. In this model, short-lived isotopes such as ^{8}Li and ^{8}B play an important role in the subsequent synthesis of heavier elements. Neutron and proton capture reactions involving ^{8}Li may also be important in initial stage of the Type-II supernovae [3], where they can produce seed nuclei for the r-process. Also, in a very high neutron density environment, neutron-induced three-particle interactions can be an alternative way to synthesize ^{12}C via the ^{8}Li produced in the reaction sequence ^{4}He(2n,γ)^{6}He(2n,γ)^{8}He(β^+)^{8}Li [4]. In supermassive stars, *i.e.*, the first stars in the universe with high proton density and very low metalicity, alternatives ways to synthesize ^{12}C are the reaction sequences ^{7}Be(p,γ)^{8}B(α,p)^{11}C(p,γ)^{12}N(β)^{12}C and ^{7}Be(p,γ)^{8}B(p,γ)^{9}C(α,p)^{12}N(β)^{12}C. In both sequences, radioactive ^{8}B nuclei can play a crucial role.

2. The potential model

The potential model as well as ANC (Asymptotic Normalization Coefficient) are indirect methods to obtain the cross section for direct capture reactions. The idea of the ANC method is to use transfer reactions such as (d,p) or (d,n) reactions, in inverse kinematics, to extract the "asymptotic wave functions normalization coefficients" that can be related to the capture cross section. The relation between the transfer and capture reactions is given by the fact that the ANC, which normalize the cross sections for the non-resonant part of the capture reaction, is obtained from peripheral transfer reactions whose amplitudes contain the same overlap function as the amplitude of the corresponding capture reaction of interest [5]. Therefore, the ANC method is based on the assumption that capture reactions at stellar energies usually proceed through the tail of the nuclear overlap function. The amplitude of the radiative capture cross sections is then dominated by contributions from large relative distances between the participating nuclei. In the ANC method, the asymptotic coefficient is used to normalize the Whittaker function, which is used to describe the tail of the overlap function, $I_{bound}=ANC\times W_{-\eta,l+1/2}(2\kappa r)$. However, it has been shown that s-wave neutron capture, even at rather low energies, is not peripheral [6,7] and so it is necessary to use another indirect method such as the potential model to calculate the wave function of the incoming neutron or proton and the wave function for the bound system. Thus, in the potential model, it is necessary to calculate the overlap function also taking into account the internal part of the nuclear potential, $I_{bound}=S^{1/2}\times\Phi(r)$. Here, $S^{1/2}$ is the spectroscopic amplitude and $\Phi(r)$ is the wave-function which describes the bound state. Also, in the ANC method, the wave function of the incoming nuclei in the continuum, ψ_{scat}, is assumed to be due only due to the Coulomb potential. This assumption may only be true for a very peripheral capture reaction. In the potential model, the continuum wave function, ψ_{scat}, has to be calculated with a potential which includes also the nuclear interaction. Thus, the essential ingredients in the potential model are the potentials used to generate the wave functions ψ_{scat} and I_{bound}, and the normalization for the latter which is given by its spectroscopic factor. This potential model, has recently been applied in the analysis of the ^{16}O(d,p)^{17}O and ^{16}O(d,n)^{17}F transfer reactions to determine the corresponding ^{16}O(p,γ)^{17}F$_{gs}$, ^{16}O(p,γ)^{17}F$_{1st}$ and ^{16}O(n,γ)^{17}O$_{gs}$ astrophysical direct capture cross sections [8].

Based on the potential model, the direct radiative capture (DRC) of an s- and/or d-wave nucleon (proton or neutron) by a nucleus b, proceeding via E1 transition and leaving the compound nucleus c in its ground state, is given by:

$$\sigma^{E1}_{b\to c}(n,\gamma)=\frac{16\pi}{9\hbar}k_\gamma^3|\langle\psi_{scat}|O^{E1}|I_{bound}\rangle|^2, \qquad (1)$$

where $k_\gamma=\epsilon_\gamma/\hbar c$ is the wave number corresponding to a γ-ray energy ϵ_γ, O^{E1} stands for the electric dipole operator and the initial-state wave function ψ_{scat} is the incoming nucleon wave function scattered by the nucleon-nucleus potential. Here the effective charge for the neutrons used in the electric dipole operator is given by $e_{eff}=-eZ/A$, where A and Z are the atomic mass and charge of the compound nucleus.

In the low energy region of astrophysical relevance, the non-resonant part of the ^{6}Li(p,γ)^{7}Be, ^{7}Li(n,γ)^{8}Li, ^{8}Li(p,γ)^{9}Be and ^{8}Li(n,γ)^{9}Li capture reactions is dominated by the E1 radiative capture of an s-wave nucleon, or a d-wave nucleon for energies above 1.0 MeV. To calculate the non-resonant part of these capture reactions in the framework of the potential model we used the computer code RADCAP developed by Bertulani [9].

In Table I we list all the parameters of the potentials used to generate the incoming and bound wave functions. All the potentials were assumed to be a Woods-Saxon shape with geometric parameters $r_0=1.25$ and $a=0.65$ fm. The depths for the bound-state potentials were obtained by adjusting them to give the binding energy of the corresponding bound system. Details of the analysis for the neutron capture reactions ^{7}Li(n,γ)^{8}Li$_{gs,1st}$ and ^{8}Li(n,γ)^{9}Li$_{gs}$ are published in Ref. 1. The scattering potential parameters for both entrance channel spins, $s=5/2^+,3/2^+$, for the ^{8}Li(2$^+$)+n system were obtained by keeping the same volume integral per nucleon, J_V/A, as those for the entrance channel spins, $s=2^+,1^+$, deduced from the scattering potentials of the ^{7}Li+n system [7]. The scattering potential depth for the

TABLE I. Wood-Saxon potential parameters used in the capture reaction calculations. Depths and B.E. are in MeV with $r_0 = 1.25$ fm and $a = 0.65$ fm, where the radii are given by $R = r_0 \times A_T^{1/3}$.

	B.E.	V_0(bound)	SF(p3/2,p1/2)	channel spin	V_0(scatt)	J_V/A (MeV/fm^3)
^{6}Li+p=^{7}Be$_{gs}$	5.606	65.25	0.83 (09),0.0	$3/2^+, 1/2^+$	46.0±2.5	678±37
^{8}Li+p=^{9}Be$_{gs}$	16.888	76.72	1.50(17),0.17(03)	$5/2^+, 3/2^+$	49.7±2.5	678±37
^{7}Li+n=^{8}Li$_{gs}$	2.033	46.38	0.87(15),0.11(2)	$2^+, 1^+$	56.15,46.50	793,657
^{7}Li+n=^{8}Li$_{1st}$	1.052	43.30	0.48,0.0	$2^+, 1^+$	56.15,46.50	793,657
^{8}Li+n=^{9}Li$_{gs}$	4.064	47.82	0.62(13),0.0	$5/2^+, 3/2^+$	58.15,48.15	793,657

^{6}Li+p system was obtained by adjusting it to reproduce the data from the ^{6}Li(p,γ)^{7}Be capture reaction [10]. Keeping the same J_V/A, we obtained the depth for the scattering potential for the ^{8}Li+p system. In this work we found that the cross sections for the capture reaction for these light nuclei are sensitive to the choice of the incoming nucleon potential. The more bound the system more sensitive the cross sections is for the choice of the potential depth used to determine the continuum wave function [13]. Although we have obtained the incoming nucleon scattering potentials for the reaction of interest from analysis of close systems, it would be interesting to obtain such potentials from direct elastic scattering measurement as ^{8}Li+p and ^{8}B+p. A program of investigation for these elastic scattering experiments at low energy is under way at the Sao Paulo University using the radioactive ion beam facility RIBRAS [11].

3. Spectroscopic factors from transfer reactions

Low-energy radioactive nuclear beams are very suitable to be used in connection with the potential model to investigate capture reactions of astrophysics interest. The Nuclear Structure laboratory at University of Notre Dame in USA [12] and later on, the Institute of Physics of Sao Paulo University [11], have developed and installed facilities to produce relatively intense low-energy and energy-resolved radiative nuclear beams RNB. Among these beams, ^{8}Li can be produced with intensities of about $\geq 10^6$ p/s in both systems. In this work we present some results on spectroscopic factors obtained from transfer reactions induced by a ^{8}Li radiative ion beam on ^{9}Be target. The experiment was performed at the Nuclear Structure Laboratory of the University of Notre Dame using the Twinsol system [12] and the procedures are described elsewhere [1,13].

We have measured angular distributions for one-neutron and one-proton transfer reactions, namely, ^{9}Be(^{8}Li,^{7}Li)^{10}Be, ^{9}Be(^{8}Li,^{9}Li)^{8}Be and ^{9}Be(^{8}Li,^{9}Be)^{8}Li reactions. Also, we have measured angular distribution for elastic scattering ^{9}Be(^{8}Li,^{8}Li)^{9}Be. From the FR-DWBA analysis, using the code FRESCO [14], for the angular distribution of these reactions, we extracted the spectroscopic factors for the ^{8}Li$\otimes$p=^{9}Be, ^{7}Li$\otimes$n=^{8}Li and ^{8}Li$\otimes$n=^{9}Li bound systems. These spectroscopic factors are listed in Table II and were used to normalize the non-resonant part of the corresponding capture reactions ^{8}Li(n,γ)^{9}Li, ^{7}Li(n,γ)^{8}Li and ^{8}Li(p,γ)^{9}Be. Transfer reactions have two vertices, and the spectroscopic factor for one of them has to be known in order to obtain the spectroscopic factor for the other vertex. In the case of the elastic-transfer reaction ^{9}Be(^{8}Li,^{9}Be)^{8}Li, where the outgoing channel is the same as the incoming channel, we have the advantage of having only one unknown vertex. In the present analysis we used the spectroscopic factor value for the ^{8}Be$_{gs}\otimes$n=^{9}Be$_{gs}$ as $S_{^9\mathrm{Be}} = 0.44(7)$, which is the average of spectroscopic factors from two (d,t) reactions studies [22,24]. The spectroscopic factor for ^{6}Li$\otimes$p=^{7}Be$_{gs}$ (J^π=$3/2^-$) vertex was considered as the average of the experimental values determined from the ^{6}Li(d,p)^{7}Li and ^{7}Li(p,d)^{6}Li reactions [28]. The spectroscopic factors for the ^{8}Li$_{gs}$ and ^{9}Li$_{gs}$ were obtained from the analysis of neutron transfer reactions ^{9}Be(^{8}Li,^{7}Li$_{gs}$)^{10}Be$_{gs}$ and ^{9}Be(^{8}Li,^{9}Li$_{gs}$)^{8}Be$_{gs}$, respectively [1]. The spectroscopic factor for the ^{8}Li$\otimes$p=^{9}Be$_{gs}$ (J^π=$3/2^-$) bound system was obtained from the analysis of the elastic-transfer ^{9}Be(^{8}Li,^{9}Be$_{gs}$)^{8}Li$_{gs}$ reaction. Details of the analysis of this particular transfer reaction will be presented elsewhere [13]. As we can see in Table-II, the spectroscopic factors obtained for the ^{8}Li$\otimes$p=^{9}Be$_{gs}$(J^π=$3/2^-$) and ^{8}Li$\otimes$n=^{9}Li$_{gs}$ (J^π=$3/2^-$) bound systems are in good agreement with shell-model calculations.

4. Capture Reactions and reaction rates

The results of the capture reaction calculations using the potential model for the ^{7}Li(n,γ)^{8}Li and ^{8}Li(n,γ)^{9}Li are shown in Fig. 1. The experimental points for ^{7}Li(n,γ)^{8}Li are from Refs. 7 and 29 to 32.The curve labeled (a; dotted line) is the sum of channel-spin $s = 1$ and $s = 2$ contributions for the neutron capture reaction to the first excited state of ^{8}Li, while curve (b; dashed line) is the sum of the channel-spin $s = 1$ and $s = 2$ contributions for the ^{8}Li ground-state. The thin solid line is the sum of these two contributions, where only the contribution of neutrons captured to the orbital $p_{3/2}$ in ^{8}Li(g.s.), using the spectroscopic factor $S_{^8Li}$(g.s.)(3/2)=0.87, is considered. The thick solid line is the same calculation considering in addition the contribution of the capture to the orbital $p_{1/2}$, using the spectroscopic factor $S_{^8Li}$(g.s.)(1/2)=0.113. For the ^{8}Li(n,γ)^{9}Li$_{gs}$ reaction, the

TABLE II. Spectroscopic factors C^2S.

	J^{π}	Shell Model calculation	(d,p),(d,n),(d,t)	This work ^{8}Li+^{9}Be transfers
$^{8}Li_{gs}\otimes n=^{9}Li_{gs}$	3/2-	$0.628^{a)}$ $0.885^{b)}$	$0.68(14)^{d)}$ $0.90^{e)}$ $0.65(15)^{f)}$	0.62 (13)
$^{7}Li_{gs}\otimes n=^{8}Li_{gs}(p_{3/2})$	2+	$0.977^{c)}$	$0.87^{g)}$	0.87 (15)
$^{7}Li_{gs}\otimes n=^{8}Li_{gs}(p_{1/2})$	2+	$0.0561^{c)}$	$0.113^{h)}$	0.113 (17)
$^{8}Be_{gs}\otimes n=^{9}Be_{gs}$	3/2-	$0.580^{c)}$	$0.44(7)^{i)}$	
$^{9}Be_{gs}\otimes n=^{10}Be_{gs}$	0+	$2.357^{c)}$	$2.23\ (13)^{j)}$	
$^{6}Li_{gs}\otimes p=^{7}Be_{gs}$	3/2-		$0.83\ (09)^{k)}$	
$^{8}Li_{gs}\otimes p=^{9}Be_{gs}(p_{3/2})$	3/2-	$1.356^{c)}$	$0.64^{i)}$	1.50 (27)
$^{8}Li_{gs}\otimes p=^{9}Be_{gs}(p_{1/2})$	3/2-	$0.153^{c)}$		0.17 (03)

a) from Ref. 15, b) from Ref. 16 using same Cohen Kurath wave-function,
c) from Cohen and Kurath [17], d) from ^{8}Li(d,p)^{9}Li reaction at 39 MeV [18],
e) from ^{8}Li(d,p)^{9}Li reaction at 76 MeV [19], f) from ^{9}Li(d,t)^{8}Li reaction at 15 MeV [20],
g) from Ref. 7, h) from Ref. 21,
i) average of S=0.37 from Ref. 22 and S=0.51 from Ref. 24, j) average of S=2.10 from Ref. 22 and S=2.356 from Ref. 23,
k) average S=0.90 [28] S=0.72 [25] S=0.87 [26], l) from the d(^{8}Li,n)^{9}Be reaction at 40 MeV [27].

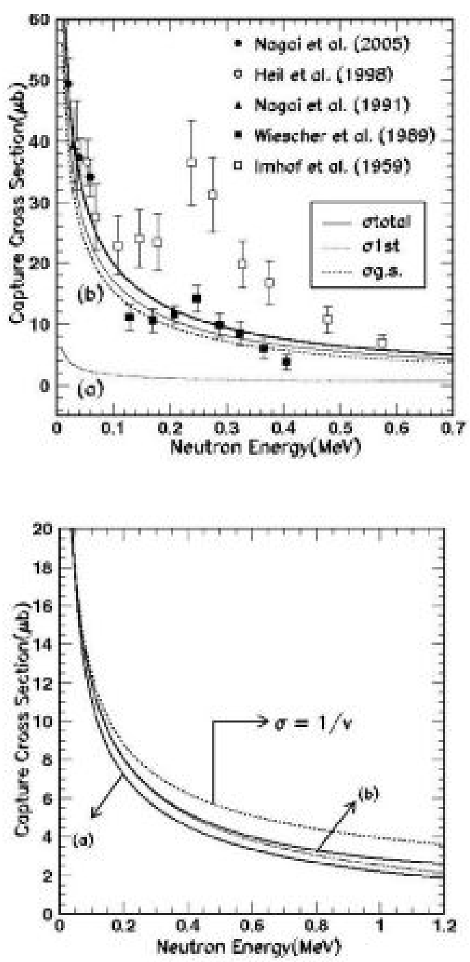

FIGURE 1. The capture cross sections for the ^{7}Li(n,γ)^{8}Li and ^{8}Li(n,γ)^{9}Li reactions. The various curves are explained in the text.

lower curves labeled (a) correspond to the potential depths scaled from the n+^{7}Li capture reaction analysis. Curves labeled (b) correspond to the assumption of the same potential for the incoming wave-function as for the bound state, for s-wave neutron only (dotted curve) and s and d-wave neutrons (solid curve). In Fig. 2 we plot the S-factor obtained for the ^{6}Li(p,γ)^{7}Be and ^{8}Li(p,γ)^{9}Be capture reactions.

We have also computed the nucleosynthesis reaction rate as a function of the temperature for the direct ^{8}Li(n,γ)^{9}Li$_{gs}$ and ^{8}Li(p,γ)^{9}Be$_{gs}$ capture reactions. The expression for the reaction rate for E1 capture in cm^{3}mol^{-1}s^{-1} is given by [33]:

$$N_A\langle\sigma v\rangle = K\int_0^{\infty}\sigma(E)E\exp(-C_2E/T_9)dE, \qquad (2)$$

where

$$K = C_1\mu^{-1/2}T_9^{-3/2}$$

and $C_1 = 3.7313\times10^{10}$, $C_2 = 11.605$, N$_A$ is Avogadro's number, μ is the reduced mass of the system, T_9 is the temperature in units of 10^{9} K, σ is the capture cross section, v is the relative velocity, and E is the energy in the center-of-mass system. E is given in MeV and the cross section in $barns$.

Although some resonances above the ^{8}Li+n and ^{8}Li+p threshold in ^{9}Li and ^{9}Be, respectively, could be important, in the present calculation only the direct capture to ^{9}Li$_{gs}$ and ^{9}Be$_{gs}$ is considered. The reaction rate for the ^{8}Li(n,γ)^{9}Li$_{gs}$ capture reaction at the temperature T_9=1 was deduced to be

$$N_A\langle\sigma v\rangle = (3.17\pm0.70)\times10^{3}\text{cm}^{3}\text{mol}^{-1}\text{s}^{-1},$$

where the uncertainty is from the uncertainty in the spectroscopic factor used in the calculation (20%) and from the variation of ±1 MeV in the potentials used to determined the distorted wave (10%). This result is comparable to the most

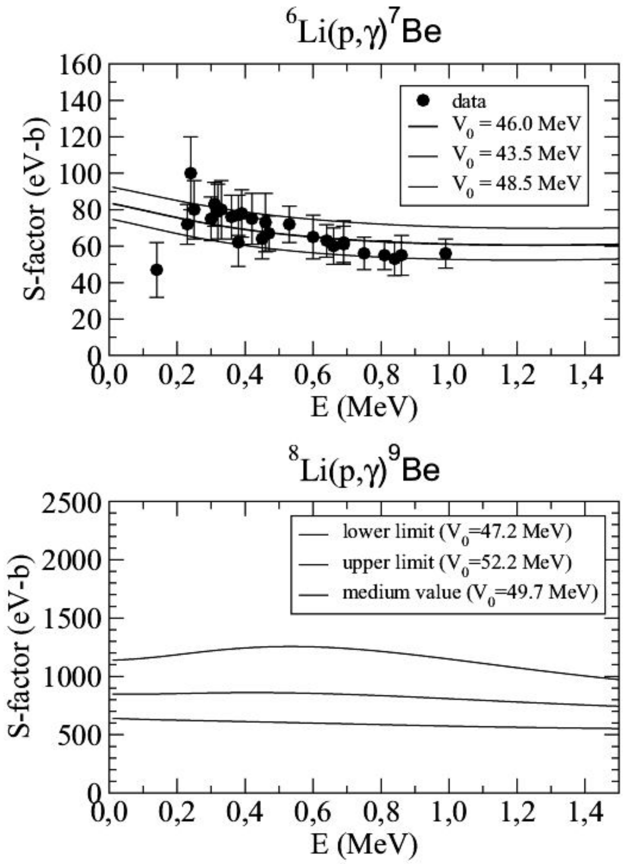

FIGURE 2. The astrophysical S-factor deduced for the ^{6}Li(p,γ)^{7}Be and ^{8}Li(p,γ)^{9}Be capture reactions. The upper and lower limits are obtained considering the uncertainties in the depth of the scattering potential.

recent theoretical calculations [34-37] and is in good agreement with the value from a recent (d,p) experiment [18]. The reaction rate for the ^{8}Li(p,γ)^{9}Be$_{gs}$ capture reaction at temperature T_9=1 was deduced to be

$$N_A\langle\sigma v\rangle = (2.2^{+0.8}_{-0.6}) \times 10^3 \mathrm{cm}^3\mathrm{mol}^{-1}\mathrm{s}^{-1},$$

where the uncertainty is from the uncertainty in the scattering potential depth and in the spectroscopic factor of $\langle^9$Be$_{gs}|^8$Li+p$\rangle$ used in the calculation. This value is about 3 times larger then the value obtained in Ref. 27.

5. Conclusion

We have measured the angular distributions for the elastic scattering of ^{8}Li on ^{9}Be and for the neutron transfer reactions ^{9}Be(^{8}Li,^{7}Li)^{10}Be and ^{9}Be(^{8}Li,^{9}Li)^{8}Be at E$_{LAB}$=27.0 MeV. Spectroscopic factors for the ^{8}Li$_{gs}\otimes$n=^{9}Li$_{gs}$ and ^{7}Li$_{gs}\otimes$n=^{8}Li$_{gs}$ bound systems were obtained from the comparison between the experimental differential cross sections and FR-DWBA calculations with the code FRESCO [14]. The spectroscopic factors obtained are compared with shell model calculations and also with experimental values from (d,p) reactions.

Using the spectroscopic factors obtained for the ^{8}Li$_{gs}\otimes$n=^{9}Li$_{gs}$ and ^{7}Li$_{gs}\otimes$n=^{8}Li$_{gs}$ bound system, we have determined the cross-sections for the ^{7}Li(n,γ)^{8}Li and ^{8}Li(n,γ)^{9}Li$_{gs}$ neutron-capture reactions based on a potential model. Our work has shown that low-energy radioactive nuclear beams can be very suitable not only to perform spectroscopic investigations but also to determine the non-resonant parts of capture reactions of astrophysical interest.

We have recently installed a double-solenoid system to produce secondary low energy radioactive ion beams at the Pelletron-LINAC laboratory in University of Sao Paulo, Brazil - The RIBRAS system [11]. This system was conceived based in the Notre Dame-Michigan *Twinsol* facility but with a higher field integral. The RIBRAS system is already operational using primary beams from the 8 MV Pelletron tandem and we are producing ^{6}He [38], ^{7}Be, ^{8}Li and ^{8}B secondary beams with intensity of about 10^4 to 10^5 particle per second. Other reaction studies using a ^{8}B beam with astrophysical interest, such as ^{8}B(α,p) are planned.

Acknowledgments

The authors wish to thank the Fundação de Amparo a Pesquisa do Estado de São Paulo (FAPESP 2006/00629-2 and 2007/06705-5) for financial support. This work was also funded in part by the U.S. NSF under Grants No. PHY03-54828 and INT03-05347.

1. V. Guimarães *et al*, *Phys. Rev. C* **75** (2007) 054602.
2. R.A. Malaney and W.A. Fowler, *Astrophys. J.* **333** (1989) 14.
3. M. Terasawa *et al.*, *Astrophys. J.* **562** (2001) 470.
4. J. Gorres, H. Herndl, I.J. Thompson, and M. Wiescher, *Phys. Rev. C* **52** (1995) 2231.
5. C.A. Gagliardi *et al. Eur. Phys. J. A* **13** (2002) 227.
6. A. Mengoni, T. Otsuka, and M. Ishihara, *Phys. Rev. C* **52** (1995) R2334.
7. Y. Nagai *et al.*, *Phys. Rev. C* **71** (2005) 055803.
8. M. Assunção, R. Lichtenthaler, V. Guimarães, A. Lepine-Szily, and A.M. Moro. Pos(NIC-IX-2006), *Proceedings of Science* (2006) 071; and *Phys. Rev. C* **70** (2004) 054601.
9. C.A. Bertulani, *Comput. Phys. Commun.* **156** (2003) 123.
10. Z.E. Switkowski *et al. Nucl. Phys.* **A 331** (1979) 50.
11. R. Lichtenthaler, A. Lepine-Szily, V. Guimaraes, G.F. Lima, and M.S. Hussein, *Eur. Phys. J.* **25** (2005) 733.
12. F.D. Becchetti *et al.*, *Nucl. Instr. and Methods in Res. A* **505** (2003) 377.
13. V. Guimarães *el al.* (to be published).

14. I.J. Thompson, *Comp. Phys. Rep.* **7** (1988) 167; and www.fresco.org.uk.
15. P. Navratil, *Phys. Rev. C* **70** (2004) 054324.
16. H. B. Jeppesen *et al.*, *Phys. Letters B* **635** (2006) 17.
17. S. Cohen and D. Kurath, *Nucl. Phys. A* **101** (1967) 1.
18. Z.H. Li *et al.*, *Phys. Rev. C* **71** (2005) 052801-R.
19. A.H. Wuosmaa *et al.*, *Phys. Rev. Lett.* **94** (2005) 082502.
20. R. Kanungo, *et al.*, *Phys. Lett.* **B 600** (2008) 26.
21. L. Trache *et al. Phys. Rev. C* **67** (2003) 062801.
22. S.E. Darden, G. Murillo, and S. Sen, *Nucl. Phys. A* **266** (1976) 29.
23. D.L. Powell, G.M. Grawley, B.V.N. Rao, and B.A. Robson, *Nucl. Phys. A* **147** (1970) 65.
24. W. Fitz, R. Jahr and R. Santo, *Nucl. Phys. A* **101** (1967) 449.
25. I.S. Towner, *Nucl. Phys. A* **126** (1969) 97.
26. B. Fagerstrom, J. Kallne, O. Sundberg, and G. Tibell, *Phys. Scr.* **13** (1976) 101.
27. J. Su *et al.*, *Chin. Phys. Lett.* **23** (2006) 55.
28. J.P. Schifer *et al.*, *Phys. Rev.* **164** (1967) 164.
29. M. Heil, F. Kaeppeler, M. Wiescher, and A. Mengoni, *Astrophys. J.* **507** (1998) 997.
30. Y. Nagai, *et al. Astrophys. J.* **381** (1991) 444.
31. M. Wiescher, R. Steininger, and F. Kappeler, *Astrophys. J.* **344** (1989) 464.
32. W.L. Imhof *et al.*, *Phys. Rev.* **114** (1959) 1037.
33. C. Angulo *et al.*, *Nucl. Phys. A* **656** (1999) 3.
34. F.K. Thielemann, J.H. Cowan, and M. Wiescher, in *Nuclei in the Cosmos*, edited by H. Oberhummer, *et al.* (Springer, Berlin, 1991).
35. P. Descouvemont, *Astrophys. J. Lett.* **405** 518 (1993).
36. T. Rauscher, J.H. Applegate, J.J. Cowan, F.K. Thielemann, and M. Wiescher, *Astrophys. J.* **429** (1994) 499.
37. C.A. Bertulani, *J. Phys. G* **25** (1999) 1959.
38. E.A. Benjamim *et al.*, *Phys. Lett. B***647** (2007) 30.